Debye classes in $A15$ compounds

J.-L. Staudenmann and B. DeFacio*
Ames Laboratory—U.S. Department of Energy and Department of Physics, Iowa State University, Ames, Iowa 50011
L. R. Testardi
NASA Headquarters, Washington, D.C. 20546
S. A. Werner
Department of Physics, University of Missouri, Columbia, Missouri 65211
R. Flükiger
Institut fur Technische Physik, Kernforschungszentrum, D7500 Karlsruhe, West Germany
J. Muller
Department de Physique de la Matière Condensée, 32 Bd. d'Yvoy, Université de Genève, CH-1212 Genève 4, Switzerland
(Received 14 January 1981)

The comparison between electron charge-density distribution of V_3Si, Cr_3Si, and V_3Ge at room temperature leads us to study the Debye temperatures at 0 K Θ_0 from specific-heat measurements for over 100 $A15$ compounds. A phenomenological $\Theta_0(M)$, M the molecular mass, is obtained from the static scaling relation $\Theta_0(M) = aM^b$ and this organizes all of the data into *five Debye classes:* $V(V_3Si)$, *V-G*, $G(V_3Ge)$, *G-C*, and $C(Cr_3Si)$. In contrast, the Debye temperature $\Theta_0(V)$, with V as the unit-cell volume does not relate alloys as $\Theta_0(M)$ does, with the exception of the C class. This latter case leads to the surprising result $M \propto V^{-1/3}$ and to a Grüneisen constant of 1.6 ± 0.1 for all compounds of this class. In the V class where V_3Si and Nb_3Sn are found, $\Theta_0(V)$ labels these two alloys differently, as does their martensitic c/a ratios. With $\bar{T}_c$ denoting the average superconducting transition temperature within a Debye class, interesting correlations are shown. One is the maximum of $\bar{T}_c$ which exists in the V class where the strongest anharmonicity occurs. Another is the case of compounds formed only by transition elements up to and including Au. This interesting case shows that $\sim 3.2 < \bar{T}_c \lesssim 5.0$ K in all of the five classes and that there is no correlation between T_c and the thermal properties. The implications of these observations for creating better models for the $A15$ compounds are briefly discussed.

I. INTRODUCTION

The $A15$ alloys are characterized by the Cr_6Si_2-type cubic structure shown in Fig. 1. The special crystallographic positions as well as the point-group symmetries are indicated. From this picture it can be seen that the Si atoms occupy the sites of a body-centered-cubic substructure and the Cr atoms form a system of three infinite, independent, mutually orthogonal chains passing through the middle of the faces. The distance between two consecutive Cr on a chain is shorter than the corresponding distance between two nearest neighbors in the pure Cr crystal and can be considered as a compression of the valence shells of the atoms on the chains. This compression has been found in all the $A15$ alloys with composition close to stoichiometry. For compounds having large deviation from stoichiometry, like $V_{0.3}Re_{0.7}$,[1] the term compression has to be redefined as a proportional average of the atomic distances constituting the chain with respect to $a/2$ where a is the lattice parameter.

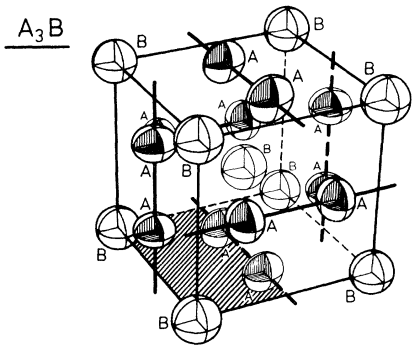

FIG. 1. The $A15$ structure (Cr_3Si-type). The shaded area represents the surface in which the electron charge-density maps are drawn.

The $A15$ compounds are known to form a very important family of more than 60 binary alloys, many of them having homogeneity domains like the V-Si (Refs. 2 and 3) and Nb-Sn (Refs. 4–6) systems; important deviations from stoichiometry have been found in V-Ir,[7,8] V-Re,[1] and Mo-Tc,[9] for example. One of the members of this family, Nb_3Ge, is characterized by the highest known superconducting transition temperature (Gavaler *et al.*,[10] Testardi *et al.*[11]).

One question which always arises when one tries to correlate T_c with the number of states at the Fermi level, the electron-phonon interaction, the lattice defect type and its amplitude, etc., is: What are the important factors to explain the relation between the superconducting transition temperature T_c and possible lattice instabilities within the $A15$ alloys? This is not the place to discuss which correlation is the most relevant since they are all related in complicated ways; instead we will show that the totality of experimental data now available possesses several remarkable regularities based on (a) the correlation between the Debye temperature[12] at 0 K, Θ_0 deduced from specific-heat measurements and the molecular mass, and (b) Θ_0 as a function of the unit cell size. Those two correlations are, of course, more closely related to the electron-phonon interaction than to any other property mentioned above. It will be shown, however, that $\Theta_0(M)$ form families which we call Debye

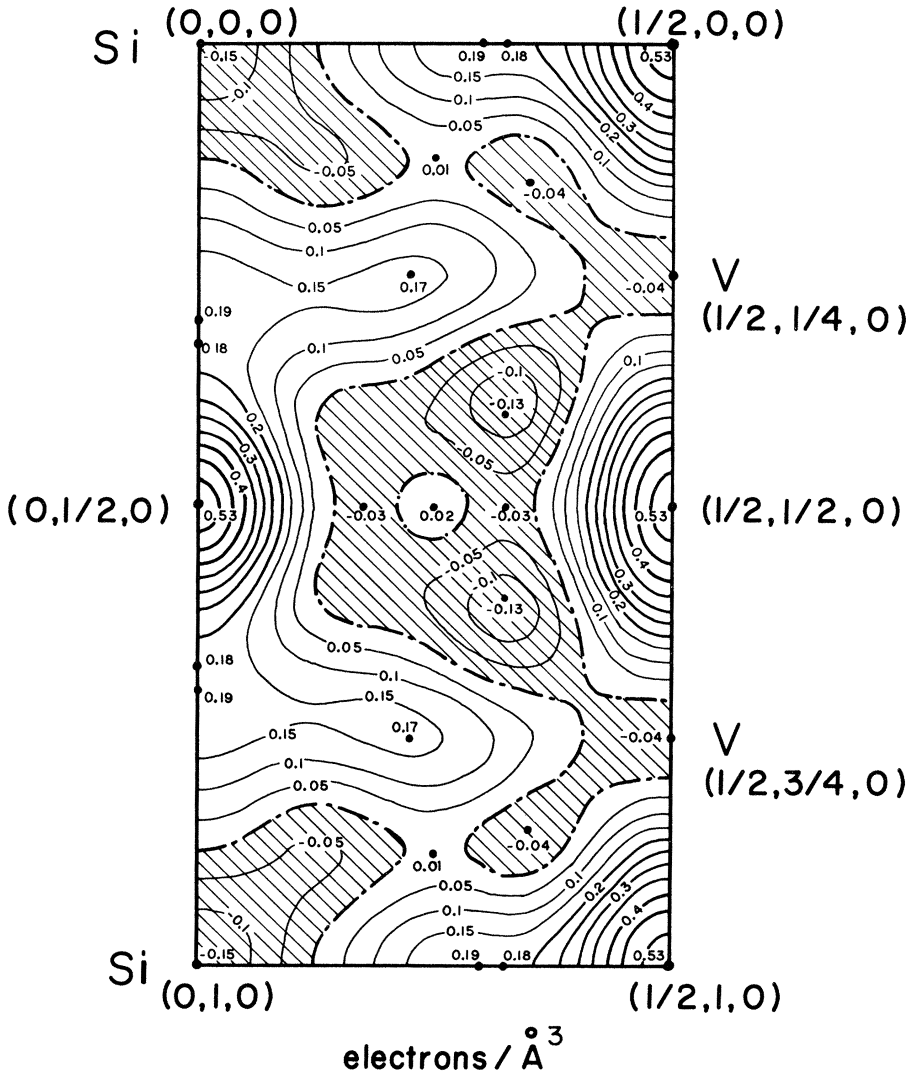

FIG. 2. Deformation electron density of V_3Si at 300 K in the (001) plane. Contours at 0.05 e Å^{-3}. Reflections up to $\sin\theta/\lambda = 0.6$ Å^{-1} are included in the Fourier transform. Negative densities are shaded. Typical standard deviation outside nuclear positions: 0.06 e Å^{-3}.

classes. On the other hand, $\Theta_0(V)$ will distinguish some peculiar differences within the same Debye class such as the c/a ratio between transforming V_3Si and Nb_3Sn alloys. At first the $\Theta_0(M)$ classification seems to have very little to do with solid-state physics while the relation $\Theta_0(V)$ enters through the Grüneisen parameter. Unfortunately, and for some reasons not yet fully understood, it has been impossible to build an overall $\Theta_0(V)$ classification with the exception of the Cr_3Si Debye class (see below and Figs. 6 and 14). However, $\Theta_0(M)$ can be related to the Debye model for harmonic vibrations [see Eq. (1)], but here we are concerned with deviations from the Debye model,[12] so such a classification simply reflects types of thermal vibrations. Since vibrations are affected by interactions between atoms present in the unit cell, a given type of thermal vibrations depends on the electronic band structure which is related to the electron charge-density distribution (referred to as ECD below) within the unit cell. This density is usually represented by a contour map where the contour levels express the electron density in electrons per cubic angstrom. The regions of interest for such maps with $A15$ compounds are the faces of the unit cell and the sections shown in Figs. 2–4 all represent the shaded surface in Fig. 1. There is no relevant information from elsewhere in the unit cell for V_3Si, Cr_3Si, and V_3Ge.

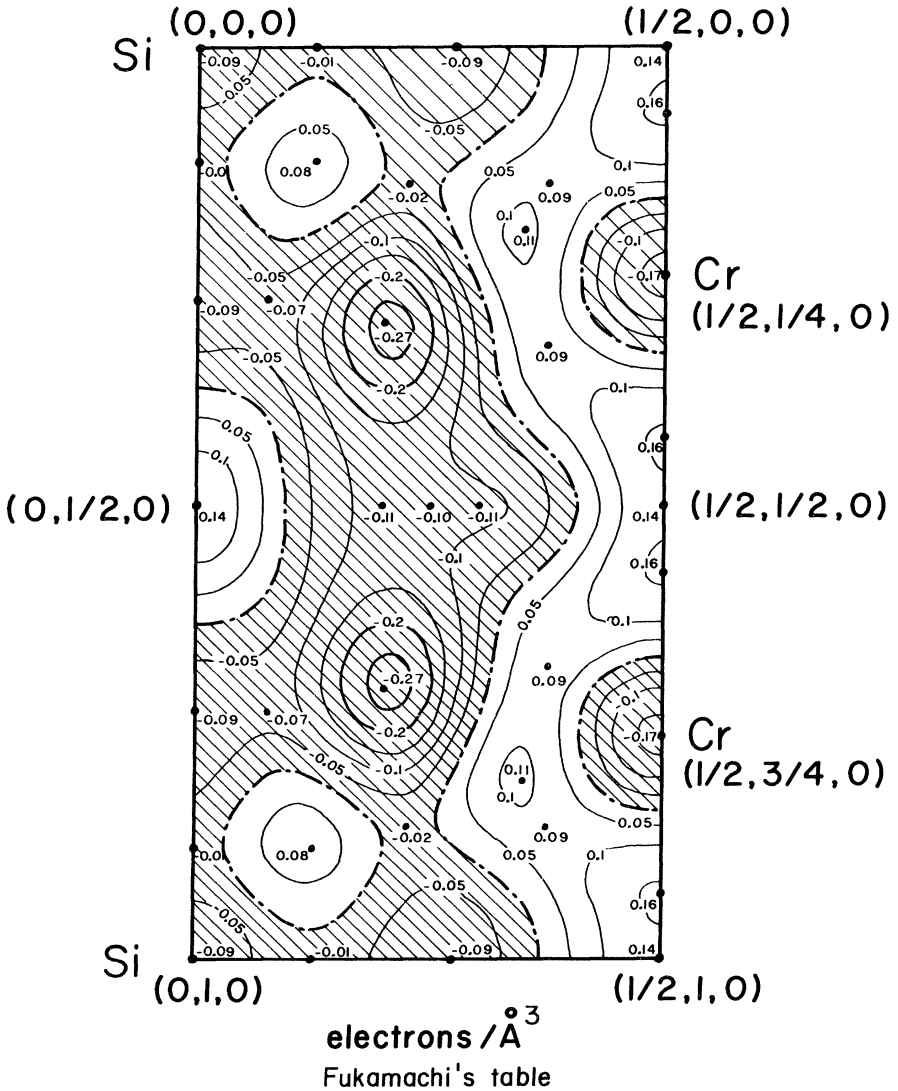

FIG. 3. Deformation electron density of Cr_3Si at 300 K in the (001) plane. Contours at 300 K in the (001) plane. Contours at 0.05 e Å^{-3}. Reflections up to $\sin\theta/\lambda = 0.6$ Å^{-1} are included in the Fourier transform. Negative densities are shaded. Typical standard deviation outside nuclear positions: 0.05 e Å^{-3}.

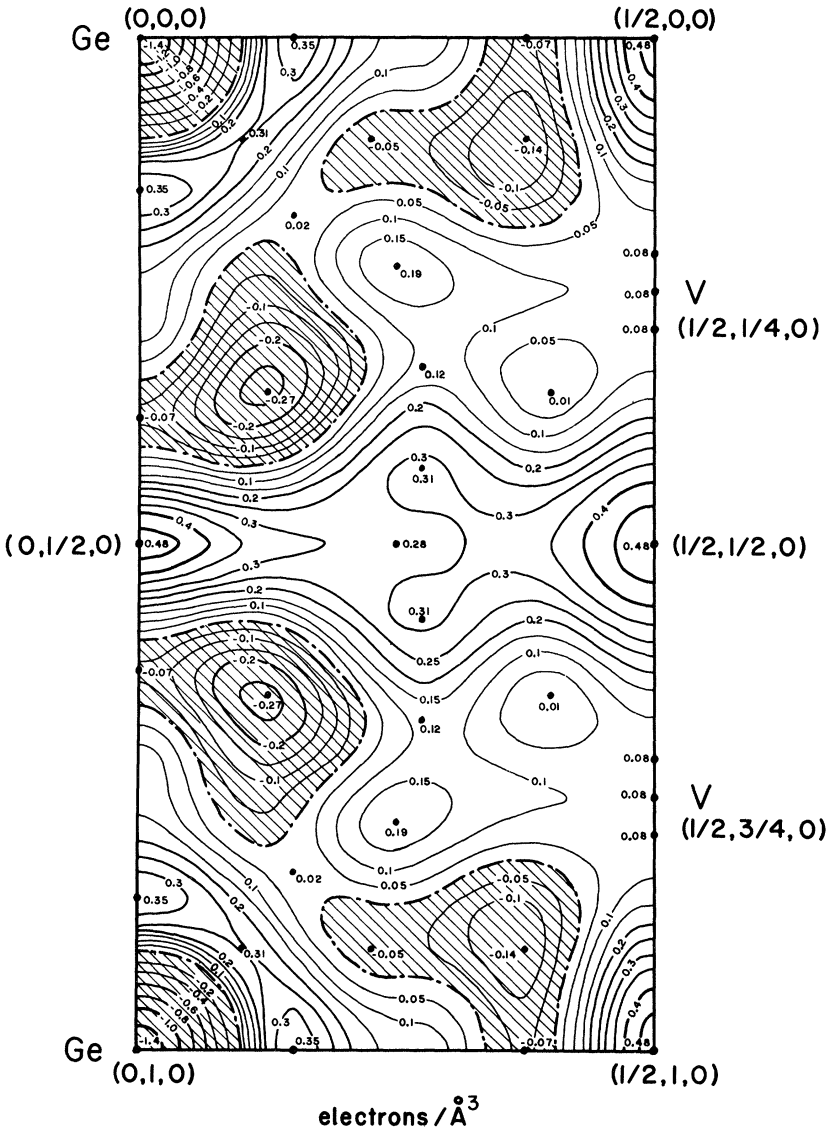

FIG. 4. Deformation electron density of V_3Ge at 300 K in the (001) plane. Contours at $0.05e$ Å^{-3}. Reflections up to $\sin\theta/\lambda = 0.6$ Å^{-1} are included in the Fourier transform. Negative densities are shaded. Typical standard deviation outside nuclear positions: $0.08e$ Å^{-3}.

II. ELECTRON DENSITY DISTRIBUTIONS IN A15

It has to be emphasized that the $\Theta_0(M)$ classification was initiated[13] in order to explain, or at least display systematically, the fundamental differences between the ECD at 300 K for V_3Si (Refs. 13 and 14) and Cr_3Si.[13,15] It is evident from the distributions shown in Figs. 2 and 3 that the main accumulation of charge found in the interatomic region is on the chain between two adjacent V or two Cr atoms [points $(0, \frac{1}{2}, 0)$, $(\frac{1}{2}, 0, 0)$, $(\frac{1}{2}, \frac{1}{2}, 0)$, and $(\frac{1}{2}, 1, 0)$ in Figs. 2–4]. The important differences between the two alloys is that the buildup of charges between two consecutive V atoms on a chain V_3Si is more than three times higher than for the same point in Cr_3Si. In fact, the difference is probably even larger. The density at the midpoint of the V-V band in V_3Si is not affected by truncation of the inverse Fourier

transform (or series). On the other hand, the density at the same point for Cr_3Si is very slowly decreasing as more and more reflections are added in the inverse process.[16] Thus, the Cr-Cr chain can be viewed as a pileup of compressed valence shells of Cr atoms without bonding. In contrast, the V-V chain seems to be made of interacting valence shells of V atoms. Another very relevant difference is the fact that the Si atoms, in V_3Si, seem to be attached to six pairs of V atoms [points $(0, \sim\frac{1}{6}, 0)$, $(0, \sim\frac{3}{4}, 0)$, $(\sim\frac{1}{6}, 0, 0)$, and $(\sim\frac{1}{6}, 1, 0)$] while, in Cr_3Si, they are directly bonded to the Cr atoms [points $(\sim\frac{1}{8}, \sim\frac{1}{8}, 0)$, $(\sim\frac{7}{8}, \sim\frac{1}{8}, 0)$ and points $(\sim\frac{1}{3}, \sim 0.2, 0)$, $(\sim 1.3, \sim 0.8, 0)$]. Based on the original $\Theta_0(M)$ plot[13] the ECD of V_3Ge at 300 K was measured. According to Fig. 4 we can see that the surroundings of the Ge atoms are intermediate to the Si atoms in V_3Si and Cr_3Si. The magnitude of the ECD density at the middle point of the V-V chain is slightly lower in V_3Ge than in V_3Si. The qualitative aspect of the V-V bond in V_3Ge is, however, quite different from that of V_3Si. We can no longer say that the Ge atoms are attached to six pairs of V atoms as in V_3Si. There the situation is similar to Cr_3Si: the Ge atoms are attached to 12 different V atoms through the pileup of charge located at points $(\sim\frac{1}{4}, \sim 1.4, 0)$ and $(\sim 1.4, \sim\frac{3}{4}, 0)$. The relatively high electron density between two different perpendicular chains came as a surprise in comparison to the corresponding ECD for the same location in V_3Si and in Cr_3Si [point $(\sim\frac{1}{4}, \frac{1}{2}, 0)$].

III. HYPOTHESIS

The ECD presented above can be consolidated into three different types of ECD. These three types constitute the starting hypothesis of this article; it is believed that the $A15$ compounds can be separated by $\Theta_0(M)$ starting with these three specific points, e.g., the one corresponding to V_3Si, V_3Ge, and Cr_3Si. Recently, during the progress of this work, three ideas have been added. Two of them are based on the large spread between the $\Theta_0(M)$ curves for the Cr_3Si and the V_3Ge Debye classes on one hand and by the large number of compounds lying between the V and G classes on the other hand. More work needs to be done in order to establish whether the existence of these two additional classes is appropriate. Finally, a remarkable universality for transition elements was discovered.

Three final introductory comments are

(a) The sorting of one particular point corresponding to each $\Theta_0(M)$ family is based on a least-squares fitting. This selection procedure may seem arbitrary, but one has to keep in mind that the Debye classes are established as a guide in order to have a better understanding of the wide range of vibrational properties of the $A15$ alloys, not to explain the individual compounds in detail. As a corollary, alloys with more than one Θ_0 will be attributed to different $\Theta_0(M)$ classes with the exceptions of V_3Si, V_3Ge, and Cr_3Si. The closest Θ_0's from specific heat to the corresponding values obtained by sound velocity measurements will be taken as reference points for V_3Si and V_3Ge.

(b) The comparison between ECD and specific heat has to be made in the following way; Debye temperatures are compared at 0 K with any ECD because the comparison has to be made where the thermal motion of the atoms is minimal. The variations of the ECD as a function of the temperature, as has been shown for V_3Si,[17–19] can be considered as a perturbation when compared to the increase of the lattice term in the specific heat. In fact, at high temperatures the Debye temperature reflects that the phonons have a non-Debye behavior; they do not follow a linear dispersion curve. In addition, the comparison would be more complicated because at room temperature most of the high T_c alloys are almost in the Dulong-Petit regime while the low T_c's are still in the intermediate range.

(c) According to the work of Schweiss *et al.*[20] and underlined by the recent publication of Junod *et al.*[21] the phonon spectrum of any $A15$ alloy has a great deal of structure. Therefore it is difficult to characterize the phonon spectrum of an $A15$ compound by only one Debye temperature. Despite this caveat, we restrict our discussion only to the Debye temperature of 0 K published in the literature and still obtain some interesting insights.

IV. DEBYE $\Theta_0(M)$ CLASSES

In 1967, Testardi and Bateman[22] published sound-velocity measurements on V_3Si single crystal. Later an article by Keller and Hanak[23] described ultrasonic velocity and attenuation data in Nb_3Sn. Keller and Hank found that the behavior of Nb_3Sn is similar to that of V_3Si. They tried and succeeded in scaling their results at all temperatures to those of Testardi and Bateman by using the static scaling relationship between the Debye temperature[12] Θ and the molecular mass M

$$\Theta \propto M^b \ , \tag{1}$$

where $b = -\frac{1}{2}$. But for sound-velocity measurements

$$\Theta \propto \bar{v} \ , \tag{2}$$

where $\bar{v}$ is the mean sound velocity. Since $\bar{v}$ depends on the elastic constants and the nature of the materials under consideration, one can write the more gen-

eral relation from ultrasonics[24]

$$\Theta \propto \left[\frac{E}{M/V}\right]^{1/2}, \tag{3}$$

where E is the elastic modulus, M is the molecular mass, and V is the unit-cell volume. As it will be shown, one would lose part of the wealth of the $A15$ specific-heat thermal data (see Table I) if M/V in Eq. (3) is replaced by the density ρ. Thus Eq. (1) will be shown to contain physics which is different from that obtained from Eq. (3). As mentioned previously, the static scaling relation in Eq. (1) between V_3Si and Nb_3Sn is valid at all temperatures. This is a strong indication that the value of the binding potential energy $U(r)$ is of the same magnitude for both compounds. Since V_3Si and Nb_3Sn have the same number of valence electrons, this strongly suggests that both alloys have the same kind of bonding, and therefore the same kind of ECD.

There is a third known ultrasonic-velocity measurement on another $A15$ alloy: V_3Ge done by Rosen, Klimker, and Weger.[25] Although the scaling procedure applies quite well for all three compounds, V_3Ge, V_3Si, and Nb_3Sn at room temperature, it fails completely when the temperature is lowered. Figure 5 exhibits the comparison of the three known ultrasonic $\Theta(T)$ functions and it is easy to see that V_3Ge cannot fit into the same category as Nb_3Sn and V_3Si. It is one of the goals of this article to show why $\Theta(M)$ does not apply for all temperatures for V_3Ge compared to the other two alloys.

It has also been shown that a similar comparison can be done on Debye temperatures from x-ray or neutron mean-square-displacement measurements of $A15$ alloys (Staudenmann,[13] Flükiger, Staudenmann, and Fisher,[26] Kodess[27]). In this particular comparison, Cr_3Si does not scale with V_3Si, Nb_3Sn, and V_3Ge. Again, this is another type of measurement which leads to significant differences among the $A15$ compounds.

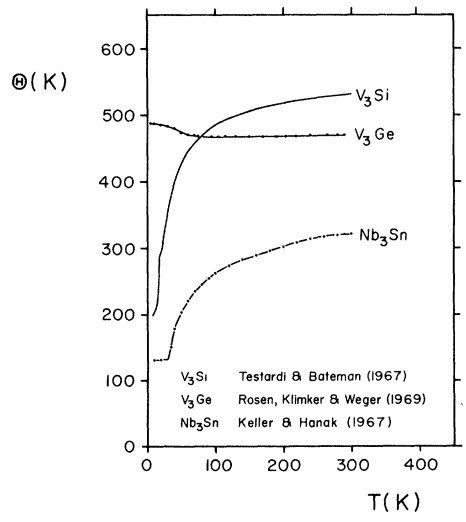

FIG. 5. Debye temperatures from sound-velocity single-crystal measurements as a function of the temperature for V_3Si, V_3Ge, and Nb_3Sn (Refs. 22, 25, and 23, respectively).

Since there are only three known ultrasonic-velocity measurements for the complete family of $A15$ alloys, and perhaps no more than a dozen elastic diffraction studies—of which only one so far includes anharmonic corrections (Staudenmann and Testardi[18,19])—it is necessary to find another consistent set of Debye temperatures. The only candidate with enough available data to be worthy of consideration is specific-heat measurements. The scaling procedure can now be extended to the complete family of $A15$ alloys if one lets the exponent b vary in relation (1). Because the scaling is based on specific-heat measurements, the result expresses a *new* correlation among the low-temperature phonon behavior of these compounds.

The interest in such a method is that it allows a classification of alloys within the same structure, that is, the complete set of Debye temperatures is split into several main categories. Each of them is represented by one curve. In the following, only five main curves are considered and are called "Debye classes" (see Sec. III).

Table I presents the complete list of the materials studied in this article. Figure 6 shows the scaling procedure applied to the different $A15$ alloys, and Table II gives the results of the different least-squares fits based on relation (1). It is surprising to see that most of the high T_c compounds are found in the same Debye class: namely, the V class. We will thus show that while large differences in the electronic density of states has been reported among the high T_c superconductors, the phonon behavior is consistently correlated through the M^{-b} factor. We also argue that the comparison between alloys not belonging to the same Debye class should be done with caution because different thermal properties must be properly accounted for.

Figure 6 also shows the limitations of the procedure. When the molecular mass is higher than 450–500 there seem to be many exceptions; $V_{0.3}Re_{0.7}$,[1] Mo_3Ir,[28] and the two Mo-Re-Pt alloys[29] are rather good superconductors. It is also expected that Ta_3Sn may be another exception.[30] The trend of the T_c increase with the molecular mass seems more pronounced for the V_3Ge Debye class than for the V_3Si class.

Table II gives the results of the least-squares fits for $\Theta_0 = aM^b$ applied to the five curves shown by Fig. 6. The Debye temperature for a given alloy has been chosen as follows; take as an example $V_{0.75}Pt_{0.25}$. Table I gives four different Θ_0 values for this alloy,

TABLE I. Complete list of the data used in this paper. The attribution of a particular alloy to a given class is based on Fig. 6.

	a (Å)	T_c (K)	V (Å^3)	M_{A_3B}	Θ_0 (K)	Debye class	Reference
$Ti_{0.75}Ir_{0.25}$	5.012	4.3	125.15	335.90	238	*V*	37
$Ti_{0.75}Ir_{0.20}Pt_{0.05}$	5.013	5.6	125.98	336.48	220	*V*	8
		5.5			209	*V*	21
$Ti_{0.75}Ir_{0.05}Pt_{0.20}$	5.025	< 1.2	126.88	338.21			8
$Ti_{0.75}Pt_{0.25}$	5.031	0.49	127.34	338.79	376	*G*	37
$Ti_{0.75}Au_{0.25}$	5.098	< 0.015	132.34	340.67	385	*G*	37
					395	*G*	38
$Ti_{0.75}Hg_{0.25}$	5.188	< 1.2	139.64	344.29	330	*G-V*	37
$Ti_{0.755}Sb_{0.245}$	5.225	5.0	142.65	263.97	282	*V*	44
	5.220	5.7	142.44	263.97	279	*V*	44
$V_{0.75}Co_{0.25}$	4.688	< 0.02	103.03	211.76	560	*G-C*	7
$V_{0.78}Ni_{0.22}$	4.708	0.4	104.35	210.60			7
$V_{0.75}Rh_{0.25}$	4.785	< 0.02	109.56	255.73	485	*G-C*	7
$V_{0.75}Pd_{0.25}$	4.825	0.08	112.33	259.23	400	*G*	7
$V_{0.29}Re_{0.71}$	4.878	8.4	116.07	587.90	409	*C*	1
$V_{0.50}Os_{0.50}$	4.808	5.2	111.15	482.28	385	*G-C*	7
$V_{0.60}Os_{0.20}Ir_{0.20}$	4.797	2.1	110.39	428.18	384	*G-C*	39
$V_{0.75}Ir_{0.25}$	4.788	< 0.02	109.77	345.03	460	*G-C*	7
					443	*G-C*	8
		< 0.02			445	*G-C*	21
$V_{0.69}Ir_{0.31}$	4.792	0.9	110.04	378.93	414	*G-C*	7
$V_{0.63}Ir_{0.37}$	4.789	1.7	109.83	412.83	395	*G-C*	7
$V_{0.778}Pt_{0.222}$	4.817	1.0	111.77	331.77	400	*G*	7
$V_{0.75}Pt_{0.25}$	4.817	3.2	111.77	347.92	511	*C*	7
		2.9			413	*G-C*	8
		2.8			415	*G-C*	39
		2.9			403	*G-C*	21
$V_{0.72}Pt_{0.28}$	4.825	1.5	112.33	365.21	471	*C*	7
$V_{0.8}Pt_{0.08}Au_{0.12}$	4.844	0.8	113.66	319.99	420	*G-C*	39
$V_{0.77}Au_{0.23}$	4.878	0.6	116.07	338.11	376	*G*	39
		2.4			354	*G*	39
$V_{0.75}Au_{0.25}$	4.882	0.8	116.36	349.79	379	*G*	7
		1.6			398	*G*	7
		2.2			387	*G*	7
					350	*G*	47
		0.6			342	*G*	21
		2.23			338	*G*	21
		2.87			332	*G*	21
$V_{0.75}Al_{0.25}$	4.829	~16.5	112.61	179.81	290	*V*	39
Film		12–13					41
$V_{0.75}Al_{0.025}Si_{0.225}$	4.733	13.9	106.03	180.80	460	*G*	39
$V_{0.80}Si_{0.20}$	4.730	9.4	105.82	185.48	475	*G*	3
$V_{0.76}Si_{0.24}$	4.726	15.1	105.56	181.83	343–348	*G-V*	3
$V_{0.75}Si_{0.25}$	4.724	16.9	105.42	180.91	280–300	*V*	3
		14.6			330	*V*	4
		16.8			465	*G*	66
					425	*G*	(not included in least squares)
$V_{0.74}Si_{0.26}$	4.723	16.3	105.35	180.00	310–320	*V*	3

TABLE I (*Continued*).

	a (Å)	T_c (K)	V (Å^3)	M_{A_3B}	Θ_0 (K)	Debye class	Reference
$V_{0.75}Al_{0.075}Ga_{0.185}$	4.826	13.0	112.40	209.72	305	*V*	39
$V_{0.82}Ga_{0.18}$	4.817	6.8	111.77	217.29	370	*G-V*	3
$V_{0.78}Ga_{0.22}$	4.820	9.8	111.98	220.29	326	*G-V*	3
$V_{0.75}Ga_{0.25}$	4.822	14.8	112.12	222.55	302	*V*	3
		14.6			310	*V*	4
		13.5			310	*V*	21
		15.1			297	*V*	21
$V_{0.73}Ga_{0.27}$	4.823	12.6	112.19	224.05	310	*V*	3
$V_{0.68}Ga_{0.32}$	4.835	4.2	113.03	227.80	363	*G-V*	3
$V_{0.75}Al_{0.05}Ge_{0.20}$	4.790	10.2	109.90	216.29	410	*G*	39
$V_{0.76}Ge_{0.24}$	4.783	6.5	109.42	224.55	415	*G*	38
		6.1			405	*G*	4
$V_{0.74}Al_{0.115}As_{0.145}$	4.783	7.3	109.42	206.65	429	*G*	39
$V_{0.77}As_{0.23}$	4.742	0.2	106.63	225.83	530	*G-C*	39
$V_{0.75}Al_{0.07}Sn_{0.18}$	4.960	4.3	122.02	245.84	328	*G-V*	39
$V_{0.80}Sn_{0.20}$	4.984	3.8	123.80	257.97	347	*G-V*	38
$V_{0.75}Al_{0.0626}Sb_{0.1875}$	4.923	4.8	119.31	250.88	434	*G*	39
$V_{0.753}Sb_{0.247}$	4.949	0.8	121.21	273.73	398	*G*	44
$V_{0.75}Pb_{0.25}$	4.937		120.33	360.02			39
$Cr_{0.72}Ru_{0.28}$	4.679	3.4	102.44	262.95	418	*G*	45
$Cr_{0.75}Rh_{0.25}$	4.674	0.07	102.11	258.89	460	*G-C*	45
$Cr_{0.72}Os_{0.28}$	4.684	4.7	102.77	362.77	442	*G-C*	45
$Cr_{0.835}Ir_{0.165}$	4.660	0.8	101.20	300.52	515	*C*	45
$Cr_{0.75}Ir_{0.25}$	4.685	0.2	102.83	348.19	449	*G-C*	45
$Cr_{0.815}Pt_{0.185}$	4.690	< 1.2	103.16	313.87	473	*G-C*	45
$Cr_{0.79}Pt_{0.21}$	4.705	< 0.02	104.16	328.18	402	*G*	45
$Cr_{0.821}Si_{0.179}$		< 1.2		190.86	740	*C*	45
$Cr_{0.75}Si_{0.25}$	4.564	< 1.2	95.07	184.07	720	*C*	45
		< 0.02			670	*C*	45
$Cr_{0.738}Si_{0.262}$	4.561	< 1.2	94.88	182.93	760	*C*	45
$Cr_{0.75}Ga_{0.25}$	4.654	< 0.3	100.80	225.71	584	*C*	45
$Cr_{0.75}Ge_{0.25}$	4.632	< 1.2	99.38	228.58	670	*C*	45
$Cr_{0.78}As_{0.22}$	4.621		98.68	228.16	448	*G*	28
$V_{0.7125}Cr_{0.375}Ai_{0.25}$	4.714	14.7	104.75	181.07			67
$V_{0.60}Cr_{0.15}Si_{0.25}$		6.5		181.54	545	*G-C*	8
	4.684	8.4	102.77	181.54			67
$V_{0.53}Cr_{0.22}Si_{0.25}$		1.2		181.84	630	*C*	8
$V_{0.375}Cr_{0.375}Si_{0.25}$		< 1.2		182.49	650	*C*	8
$V_{0.25}Cr_{0.50}Si_{0.25}$		< 1.2		183.02	650	*C*	8
$Zr_{0.75}Au_{0.25}$	5.487	< 1.2	165.20	470.63	310	*G*	38
$Zr_{0.80}Sn_{0.20}$	5.626	< 1.2	178.07	386.86	292	*G-V*	38
$Zr_{0.755}Pb_{0.245}$	5.656	< 1.2	180.54	478.53	255	*G-V*	38
$Nb_{0.75}Rh_{0.25}$	5.137	2.6	135.56	381.62	398	*G-C*	38
$Nb_{0.75}Os_{0.25}$	5.131	1.0	135.09	468.92	378	*G-C*	38
$Nb_{0.725}Os_{0.275}$	5.123	0.3	134.45	478.65	374	*G-C*	46
$Nb_{0.775}Ir_{0.225}$	5.147	0.3	136.35	460.99	374	*G-C*	46
$Nb_{0.75}Ir_{0.25}$	5.135	1.6	135.40	470.92	409	*C*	38
		1.6			378	*G-C*	8
		1.55			377–379	*G-C*	21
$Nb_{0.72}Ir_{0.28}$	5.120	2.9	134.22	480.83	362	*G-C*	46

TABLE I (*Continued*).

	a (Å)	T_c (K)	V (Å^3)	M_{A_3B}	Θ_0 (K)	Debye class	Reference
$Nb_{0.75}Ir_{0.10}Pt_{0.15}$	5.147	6.0	136.35	472.65	360	*G-C*	8
		5.95			347–352	*G-C*	21
$Nb_{0.80}Pt_{0.20}$	5.178	3.2	138.83	453.37	358	*G*	46
$Nb_{0.75}Pt_{0.25}$	5.155		136.99	473.81	350	*G*	38
		10.6			340	*G*	8
		~9			335	*G*	21
		8.9			376	*G-C*	21
		10.5			348	*G*	21
$Nb_{0.75}Pt_{0.075}Au_{0.175}$		12.9		475.12	306	*G*	8
					290	*G-V*	8
	5.193	12.7	140.04		300	*G*	38
		11.5			305	*G*	21
		12.9			290	*G-V*	21
$Nb_{0.75}Pt_{0.15}Au_{0.10}$	5.177	12.9	138.75	474.76	316–321	*G*	8 68
		11.5			316	*G*	21
		12.9			290	*G*	21
$Nb_{0.76}Au_{0.24}$	5.211	10.8	141.50	471.52	280	*G-V*	38
					280	*G-V*	39
					280	*G-V*	47
$Nb_{0.75}Au_{0.25}$	5.203	10.6	140.85	475.69	253	*G-V*	8
					253	*G-V*	39 69
		10.6			251	*G-V*	21
$V_{0.675}Nb_{0.075}Au_{0.25}$		1.4		362.28	320	*G-V*	39 47
$V_{0.5625}Nb_{0.1875}Au_{0.25}$		0.85		381.27	305	*G-V*	39 47
$V_{0.375}Nb_{0.375}Au_{0.25}$		0.9		412.74	280	*G-V*	39 47
$V_{0.1875}Nb_{0.5625}Au_{0.25}$		3.1		444.21	280	*G-V*	39 47
$V_{0.75}Nb_{0.675}Au_{0.25}$		6.6		463.10	280	*G-V*	39 47
$Nb_{0.75}Al_{0.25}$	5.182	18.3	139.15	305.70	292	*G-V*	3
	5.186	18.7	139.48	305.70	283	*V*	49
		18.6			290	*G-V*	50
		18.2			292	*G-V*	21
$Nb_{0.84}Si_{0.16}$	5.145	5.7	136.19	330.14	315	*G-V*	48
$Nb_{0.82}Si_{0.18}$	5.133	6.9	135.24	324.95	304	*G-V*	48
$Nb_{0.75}(Nb_{0.61}Si_{0.39})_{0.25}$	5.213	5.9	141.67	346.34	283	*G-V*	70
$Nb_{0.9025}Si_{0.0975}$ $Nb_{0.75}(Nb_{0.46}Si_{0.56})_{0.25}$ $(Nb_{0.865}Si_{0.135})$	5.192	3.5	139.96	336.62	269	*V*	70
$Nb_{0.76}Ga_{0.24}$	5.168	19.8	138.03	349.37	280	*G-V*	71
$Bb_{0.75}Al_{0.20}Ge_{0.06}$	5.173	20.0	138.43	314.82	278	*V*	51
		19.7			295	*G-V*	52
$Nb_{0.82}Ge_{0.18}$	5.167	6.6	137.95	357.00	345	*G*	48
$Nb_{0.755}Ge_{0.245}$	5.140	21.8	135.80	351.71	289–302	*G-V*	48
Amorphous		3.9			222		72

TABLE I (*Continued*).

	a (Å)	T_c (K)	V (Å^3)	M_{A_3B}	Θ_0 (K)	Debye class	Reference
$Nb_{0.75}(Nb_{0.92}Ge_{0.08})_{0.25}$ $(Nb_{0.98}Ge_{0.02})$	5.239	5.6	143.80	370.00	260	*V*	70
$Nb_{0.75}(Nb_{0.82}Ge_{0.18})_{0.25}$ $(Nb_{0.955}Ge_{0.045})$	5.230	4.4	143.06	367.97	271	*V*	70
$Nb_{0.75}(Nb_{0.71}Ge_{0.29})_{0.25}$ $(Nb_{0.9275}Ge_{0.0725})$	5.219	3.6	142.16	365.73	305	*G-V*	70
$Nb_{0.75}In_{0.25}$	5.303		149.13	393.54			39
$Nb_{0.86}Sn_{0.14}$	5.273	6.3	146.61	386.06	340	*G*	6
$Nb_{0.83}Sn_{0.17}$	5.278	6.3	147.03	389.16	305	*G-V*	6
$Nb_{0.81}Sn_{0.19}$	5.281	~7	147.28	391.22	305	*G-V*	6
$Nb_{0.80}Sn_{0.20}$	5.283	~8.0	147.45	392.25	307	*G-V*	5
$Nb_{0.753}Sn_{0.247}$	5.289	17.9	147.95	397.10	245	*V*	6
$Nb_{0.75}Sn_{0.25}$	5.289	18.0	147.95	397.41	238	*V*	6
		17.3			290	*G-V*	4
	5.289	18.0			228	*V*	5
		18.0			232	*V*	21
$Nb_{0.83}Sb_{0.17}$	5.260	2.0	145.53	391.24	345	*G*	44
$Mo_{0.40}Tc_{0.60}$	4.935	13.2	120.19	351.10	349	*G*	9
$Mo_{0.525}Re_{0.46}Pt_{0.015}$	4.974	11.7	123.06	555.79	355	*G-C*	29
$Mo_{0.6}Re_{0.35}Pt_{0.05}$	4.973	9.8	122.99	529.95	365	*G-C*	29
$Mo_{0.75}Os_{0.25}$	4.969	12.7	122.69	478.02	380	*G-C*	28
$Mo_{0.75}Ir_{0.25}$	4.970	8.4	122.76	480.02	452	*C*	28
		8.5			325	*G*	4
$Mo_{0.81}Pt_{0.19}$	4.989	4.7	124.18	459.11	390	*G-C*	73
$Mo_{0.765}Al_{0.235}$	4.950	0.4	121.29	318.94	500	*C*	28
$Mo_{0.762}Si_{0.238}$	4.893	1.7	117.15	319.16	538	*C*	28
$Mo_{0.75}Ga_{0.25}$	4.944		120.85	357.54			39
$Mo_{0.762}Ge_{0.238}$	4.935	1.7	120.26	361.53	476	*C*	28
$Mo_{0.75}Sn_{0.25}$	5.094		132.18	406.51			39

TABLE II. Results of the least-squares fits to $\Theta_0 = aM^b$. *V* stands for the V_3Si Debye class, *G* for the V_3Ge class, and *C* for the Cr_3Si class. The two intermediate classes (*V-G* and *G-C*) have been added because of the large intervals between the *V* and *G* classes on one hand and between the *G* and *C* classes on the other hand. Total number of alloys: 110.

Class	a	b	r^2	No. alloys
V	1367.53	−0.286	0.566	16
V-G	1725.51	−0.297	0.710	26
G	3026.37	−0.361	0.848	25
G-C	5020.13	−0.421	0.920	26
C	8482.63	−0.483	0.905	17

one higher than the three others. The higher value is taken alone and put in a given class while the three others are averaged and attributed to another class. The reduced statistical r^2 is unity/zero for complete/zero correlation. An r^2 value of about 0.7 is usually considered as the signature of a reasonable fit. It can be seen (Table II) that the r^2 value for the Debye class of V_3Si is marginal. This suggests that the simple model given by formula (1) is not sufficient and that a correction term is needed. On the other hand, the four other r^2 values seem to adequately describe the vibrational behavior of the four other Debye classes.

We wish to stress that the Debye class of V_3Si has the strongest departure from the $M^{-1/2}$ behavior. This can be explained by anharmonicity of the atomic vibrations in each cell unit. Therefore the average superconducting temperature $\bar{T}_c$ is a maximum where the anharmonic contribution is maximum as emphasized many times by one of us[31] (see Table III).

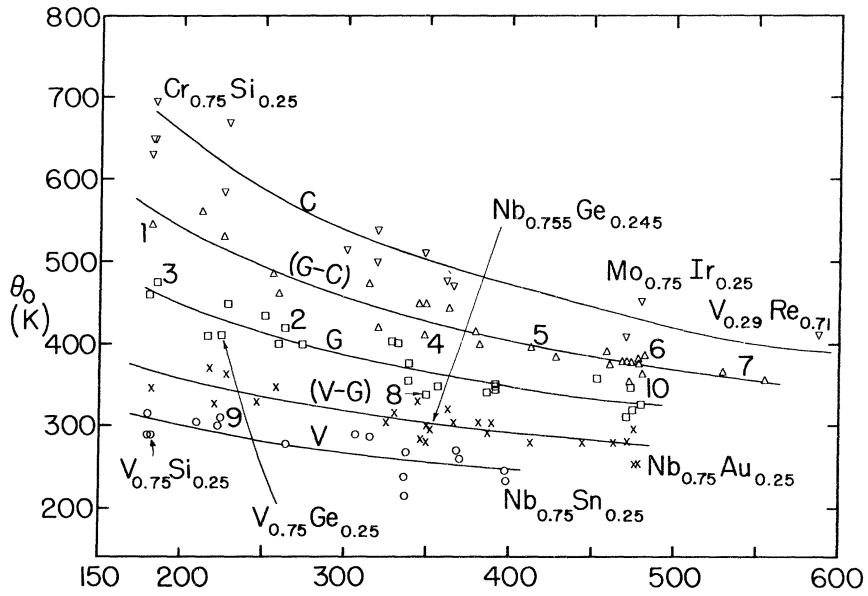

FIG. 6. Debye temperatures at 0 K from specific-heat measurements (see Table I) as a function of the molecular mass. These Θ_0 temperatures are distributed (see text) in fives classes: *V* stands for the V_3Si class, *G* for the V_3Ge class, and *C* for the Cr_3Si class; *V-G* and *G-C* are intermediate classes based only on the large intervals between the first three classes. The numbers 1 to 10 refer to the following compounds: $V_{0.60}Cr_{0.15}Si_{0.25}$, $Cr_{0.72}Ru_{0.28}$, $V_{0.80}Si_{0.20}$, $V_{0.75}Pt_{0.25}$, $V_{0.63}It_{0.37}$, $V_{0.50}Os_{0.50}$ (the closest point on the left is $Mo_{0.75}Os_{0.25}$), $Mo_{0.60}Re_{0.35}Pt_{0.05}$ (left) and $Mo_{0.525}Re_{0.46}Pt_{0.015}$ (right of the number 7), $V_{0.75}Au_{0.25}$, $V_{0.73}Ga_{0.27}$, and $V_{0.75}Ga_{0.25}$ (closer to the *V* Debye class line), and finally $Nb_{0.75}Pt_{0.25}$ (square between the *G* and *G-C* curves). $Mo_{0.40}Tc_{0.60}$ is the upper square of the three squares grouped on the *G* curve, the lowest one is $Nb_{0.83}Sb_{0.17}$.

TABLE III. $\bar{T}_c$ = average of the superconducting transition temperature T_c for alloys belonging to a given class. Numbers in parentheses are standard deviations. An individual T_c is chosen as being the maximum T_c per class (for example $Nb_{0.75}Pt_{0.075}Au_{0.175}$ has a T_c of 12.9 K in the *G* class, see Table I). No. represents the number of T_c's (alloys) included in the average. This table is divided into three main columns: (a) all compounds belonging to a given class, (b) alloys where the two (or more) components are transition metals (including Au), and (c) compounds where the *B* part of A_3B is composed of nontransition elements. *V* stands for the V_3Si Debye class, *G* for the V_3Ge class, and *C* for the Cr_3Si class. The two intermediate classes (*V-G* and *G-C*) have been added because of the large intervals between the *V* and *G* classes on one hand and between the *G* and *C* classes on the other hand.

	$A15-A_3B$					
	All members		*B* = Transition element		*B* = Nontransition element (up to Au)	
Debye class	$\bar{T}_c$ (K)	No.	$\bar{T}_c$ (K)	No.	$\bar{T}_c$ (K)	No.
V	12.1(6.0)	16	5.0(0.7)	2	13.1(5.7)	14
V-G	6.8(5.7)	26	5.9(4.8)	8	7.2(6.1)	18
G	5.1(4.6)	25	4.2(4.8)	14	6.2(4.1)	11
G-C	3.4(3.8)	26	3.2(3.8)	25	6.5	1
C	1.7(2.6)	17	4.0(3.3)	6	0.5(0.7)	11

V. $\Theta_0(V)$ CHARACTERIZATION

The Grüneisen constant[32] is related to the Debye temperature Θ_0 and to a reference volume V—usually the volume of the unit cell—by the following formula

$$\gamma_G = -\frac{d(\ln\Theta_0)}{d(\ln V)} = -\frac{V d\Theta_0}{\Theta_0 dV} \quad . \tag{4}$$

γ_G gives an estimate of anharmonic vibrations in crystals. In a plot of the Debye temperature as a function of the volume, one can distinguish three different conditions:

(i) $\gamma_G > 0$ or a negative slope. This is the case of a normal anharmonic behavior. An increase in V is translated into a softening of the vibration, i.e., a decrease in Θ_0. Conversely, a decrease in V (compression) results in a hardening of the vibration, i.e., an increase in Θ_0.

(ii) $\gamma_G = 0$ or a zero slope. This corresponds to the *harmonic* case; vibrations do not reflect any change in volume or compression.

(iii) $\gamma_G < 0$ or a positive slope. This strange behavior is anomalous for solids because a decrease in volume induces a softening and a decrease in compression generates a hardening.

One way of changing the volume is to apply a stress to the material being studied and measure the Debye temperature (see for instance Ref. 33). Another way is to vary the volume by changing the concentration. This second possibility is, of course, only valid in the presence of a homogeneity domain within the same crystallographic phase. The second model described here is not equivalent to the stress technique because the chemistry is changed in a fundamental way. Though it is important to be aware that in anharmonic solids the stress technique may induce hybridization as well as valence fluctuations; under these conditions, the chemistry may also be changed. We are convinced that the stress technique is better than the volume variation by changing the concentration, but there are very few examples in which the stress method has been studied.[31,34] Therefore, we believe that despite this reservation, the volume variation by changing the concentration will give a fair estimate of anharmonic vibrations in a given class (see conclusions for the Cr_3Si Debye class). Before reviewing some $A15$ systems, we would like to mention that the lattice parameters reported in Table I were all measured at room temperature. For instance, $a = 4.718$ Å for V_3Si at 78 K as well as at ~ 24 K: by comparison, $a = 4.724$ Å for the room-temperature determination[17–35]; such a small variation will be of no consequence for our purpose. Note that differences of the same order have been published for Nb_3Sn.[36]

VI. COMPARISON OF $\Theta_0(M)$ AND $\Theta_0(V)$ FOR SOME $A15$ SYSTEMS

A. $Ti_{0.75}$-$X^T_{0.25}$, X^T = Ir, Pt, Au, Hg; Refs. 8, 37, and 38

In this system of binary and pseudobinary alloys, $\Theta_0(V)$ scales $\Theta_0(M)$ quite well. By this we mean that the shape of the two curves is roughly the same, and the relation between the two curves is approximately constant. This includes cases where the two functions with the same shape are translated along either their "x axis" or "y axis." Although the molecular mass and the volume of the unit cell are two components of the density, we keep them as two independent variables for reasons which will become clear. The maximum of $T_c = 5.6$ K corresponds to a minimum in Θ_0 ($Ti_{0.75}Ir_{0.20}Pt_{0.05}$). There is a stabilization of the Debye temperature between Pt and Au, and then a sudden softening of $Ti_{0.75}Hg_{0.25}$.

B. V-X^T, X^T = Re, Os, Ir; Refs. 1, 7, 8, and 39

Despite the dramatic changes in the concentration of the components in the alloys shown in Fig. 7, one can see that $\Theta_0(M)$ and $\Theta_0(V)$ scale together rather well. In this system the trend toward a T_c increase is on the positive slope on the right-hand side of the picture. As already mentioned, alloys with molecular mass higher than 500 seem to be favorable to superconductivity. If this trend continues, one might expect V-W to be an even better superconductor that $V_{0.3}Re_{0.7}$ with a formula close to $V_{0.1}W_{0.9}$.

C. V-X^T, X^T = Ir, Pt, Au; Refs. 7, 9, and 39

This system can probably not be understood in terms of a unique behavior, but rather as the super-

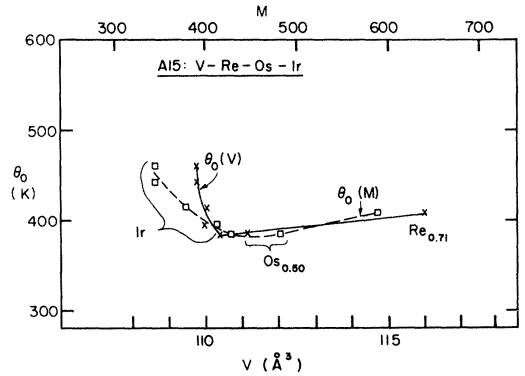

FIG. 7. $\Theta_0(M)$ and $\Theta_0(V)$ for the $A15$ phase of V-X^T systems where X^T = Re, Os, and Ir. Note that X^T can be a mixture of elements.

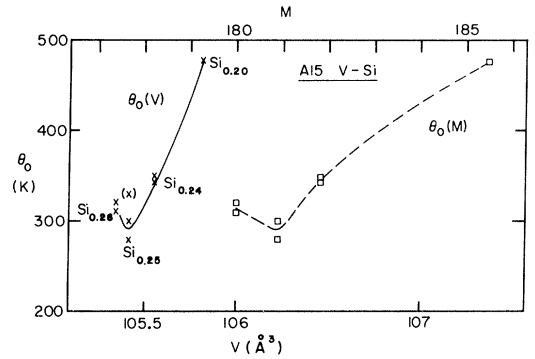

FIG. 8. $\Theta_0(M)$ and $\Theta_0(V)$ for the $A15$ phase of the V-Si homogeneity domain.

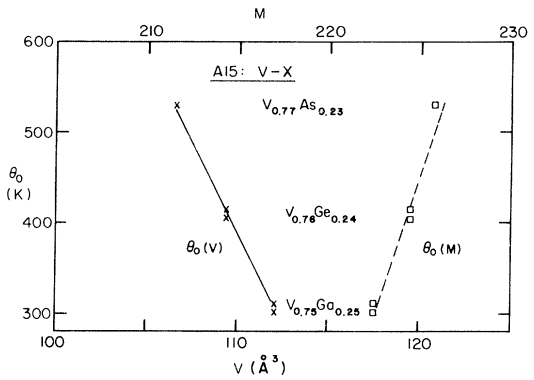

FIG. 9. $\Theta_0(M)$ and $\Theta_0(V)$ for the $A15$ phase of V-X systems where X = Ga, Ge, and As.

position of three different ones V-Ir-Pt, V-Pt (-Au), and V(-Pt)-Au. In order to have a better understanding of these different trends, one needs many more data points.

D. V-X, X = Si, Ge, Sn; Refs. 3, 4, and 38

The hardening of V_3Ge as compared to V_3Si and V_4Sn cannot be explained yet. Without additional points, this system has to be understood as composed of two different regimes.

E. V-Si; Refs. 3 and 4

Figure 8 shows the $\Theta_0(M)$ and $\Theta_0(V)$ dependence in the $A15$ phase in the V-Si (Refs. 3 and 40) system. One immediately notes that both curves scale each other. In addition, $V_{0.75}Si_{0.25}$ is in a minimum with negative γ_G for concentrations lower than 25% of Si. Note that concentrations lower than 25% of Si result in larger masses and larger volumes. It means that a V-Si alloy has a trend towards instability which increases when its concentration goes from 20% to 25% of Si. A minimum in $\Theta_0(V)$ as well as in $\Theta_0(M)$ for such a system can be understood in terms of possible lattice instabilities.[22,31]

F. V-Al-Si; Refs. 39, 41, and 42

Physical properties of V_3Al were first obtained by extrapolation techniques (see Flükiger[39] and Dew-Hughes[42]). Later Hartsough and Hammond[41] and then Testardi *et al.*[40] found a high T_c in V_3Al films. The Debye temperature used for V_3Al is the one obtained by Flükiger[39] and is an extrapolation.

This system is first described here, which justifies the fact that M and V have to be kept as two independent parameters; the behavior of $d\Theta_0(M)/dM$ does not have the same sign as $d\Theta_0(V)/dV$. This behavior seems to occur frequently in pseudobinary systems.

G. V-X, X = Ga, Ge, As; Refs. 3, 4, 38, and 39

These three binary compounds are presented in Fig. 9. It is again easy to see the sign change from $\Theta_0(V)$ to $\Theta_0(M)$. In this figure the two lines have to be considered as a guide to the eye, because measurements with intermediate composition between Ga, Ge, and As are not available.

H. V-Ga; Refs. 3 and 4

Figure 10 exhibits the behavior of $\Theta_0(M)$ and $\Theta_0(V)$ for the V-Ga $A15$ system.[3] In this particular case the γ_G's are found to be opposite to these for the V-Si alloys since concentrations of lower than 25% of Ga result in lower volumes as well as lower

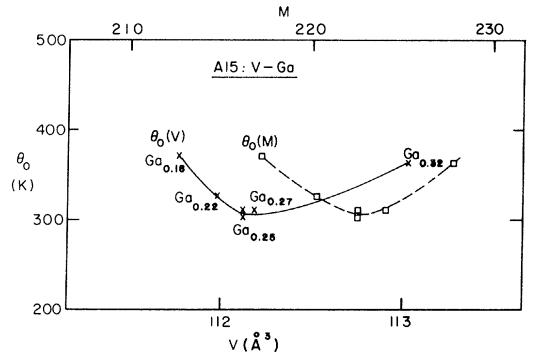

FIG. 10. $\Theta_0(M)$ and $\Theta_0(V)$ for the $A15$ phase of the V-Ga homogeneity domain.

masses (see Sec. V E). This clearly shows that the main component of the stability is different for these two systems. As for $V_{0.75}Si_{0.25}$, a minimum in both $\Theta_0(M)$ and $\Theta_0(V)$ is also found in $V_{0.75}Ga_{0.25}$. Microscopic work below 50 K by Nembach and Tachikawa[43] on $V_{0.75}Ga_{0.25}$ obtained by coating 25-μm-thick and 10-mm-wide cold-rolled vanadium tapes with gallium at $\sim 800\,^{\circ}C$ seems to indicate the possibility of a martensitic transition. Unfortunately, this potential result has never been demonstrated on bulk samples. Despite this, the minimum of Θ_0 for the V-Ga system can still be understood as a trend toward incipient instability.

I. V-Al-X, X = Ga, Ge, As, Sn, Sb; Refs. 3, 4, 27, 38, 39 and 44

When X = Ga, Ge, and As, one observes the strange case where the slope of Θ_0 as a function of the volume is negative, and the slope of $\Theta_0(M)$ is positive. But for X = Sn and Sb, it is found that $\Theta_0(V)$ and $\Theta_0(M)$ scale each other.

J. Cr-X^T, X^T = Os, Ir, Pt; Ref. 45

Here, one would see two different scaling modes, one for X^T = Os and Ir and the other for Pt.

K. Cr-X, X = Ga, Ge, As; Refs. 28 and 45

If pseudobinary alloy specific-heat data become available, one will probably find two regimes: the first between Cr_3Ga and Cr_3Ge where $\Theta_0(V)$ does not scale $\Theta_0(M)$, and the second between Cr_3Ge and $Cr_{0.78}As_{0.22}$ where the two curves scale each other.

L. Nb-X^T, X = Os, Ir, Pt, Au; Refs. 8, 38, 39, 46, and 47

The four possible binary systems represented in Fig. 11 are characterized by a change of sign between $d\Theta_0(M)/dM$ and $d\Theta_0(V)/dV$ within their homogeneity domain. The same systems based on V metals do not show this behavior, but exhibit normal scaling between $\Theta_0(M)$ and $\theta_0(V)$. In addition, one can see that the Nb-Os alloys are found on the same curve with the Nb-Ir compounds. For these systems, the behavior of $\Theta_0(V)$ is simpler than $\Theta_0(M)$, with the exception of the angle made by $Nb_{0.75}Pt_{0.075}Au_{0.175}$, $Nb_{0.76}Au_{0.26}$, and $Nb_{0.75}Au_{0.25}$; there the line joining those three points may not be correct.

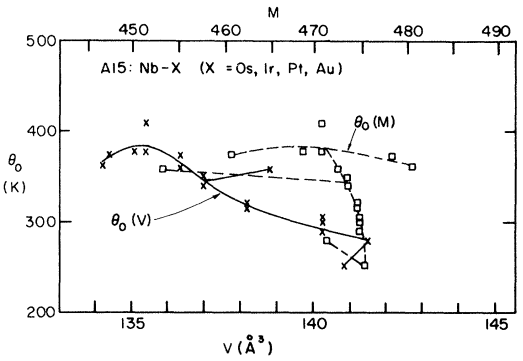

FIG. 11. $\Theta_0(M)$ and $\Theta_0(V)$ for the $A15$ phase of Nb-X^T systems where X^T = Os, Ir, Pt, and Au. Note that X^T can be a mixture of elements.

M. Nb-X, X = Si, Ge, Sn; Refs. 3–6, 21, 32, and 48

To study the Nb-based $A15$ alloys, Fig. 12 compares the following systems: Nb-Si, Nb-Ge, and Nb-Sn. Again it can be seen that the $\Theta_0(M)$ and $\Theta_0(V)$ functions scale each other very well. The situation concerning the homogeneity domains is somewhat different than for the two V-base alloys discussed above: it only concerns concentrations lower than 25% of the B component of the alloy. Even with this restriction on concentration, one sees immediately that the Nb-Si (Ref. 48) and Nb-Ge (Ref. 48) phases have similar behavior to the one of the V-Si (Ref. 3) system, while the Nb-Sn (Refs. 5 and 6) alloys are comparable only to the one of V-Ga (Ref. 3). This very simple difference between the two $\Theta_0(V)$ behaviors for the V-Si and Nb-Sn systems could very well be a part of the explanation of the differing c/a ratio for the two martensitic phases. This also implies that the anharmonic properties cannot be identi-

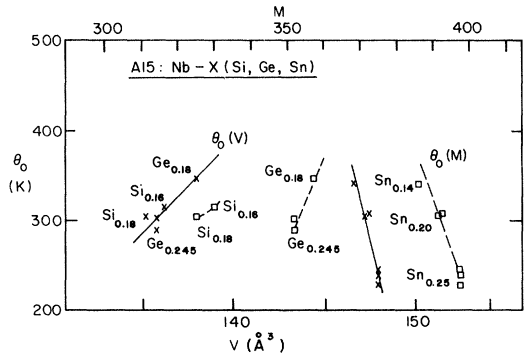

FIG. 12. $\Theta_0(M)$ and $\Theta_0(V)$ for the $A15$ phase of Nb-X homogeneity domains where X = Si, Ge, and Sn.

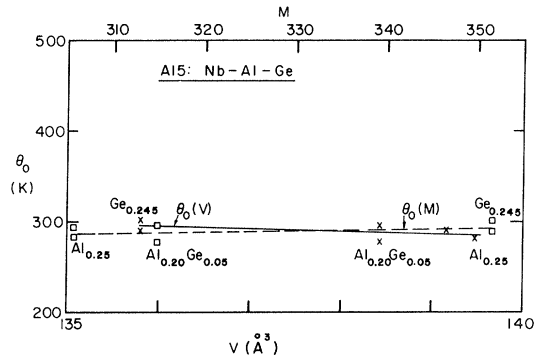

FIG. 13. $\Theta_0(M)$ and $\Theta_0(V)$ for the $A15$ phases of the Nb-Al-Ge systems.

cal to that of V_3Si when the softening of the vibrations is taking place. This is in agreement with the fact that dE'/dp are opposite for V_3Si and Nb_3Sn, where E' is the elastic modulus and p an hydrostatic pressure.[33,34] As far as the systems Nb_3Si, Nb_3Ge, and Nb_3Sn are concerned, one can draw lines between alloys on Fig. 12 and find that $\Theta_0(M)$ and $\Theta_0(V)$ scale to each other well, in contrast to observations for the V-based related systems.

N. Nb-Al-Ge; Refs. 48–59

To complete this discussion on particular $A15$ systems, we would like to mention that the pseudobinary Nb-Al-Ge system has, surprisingly, an harmonic behavior as far as the $\Theta_0(V)$ relationship is concerned, but a reverse correspondence when $\Theta_0(M)$ is compared to $\Theta_0(V)$ (see Fig. 13).

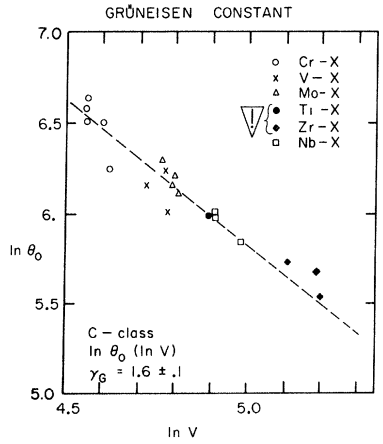

FIG. 14. $\ln\Theta_0$ ($\ln V$) plot for the alloys in the C class. The Zr-based compounds have been added on the figure as well as Ti_3Au because they happen to fit the same straight line. The symbol ▼ means that these four points are not included in the least-squares fit.

O. $\Theta_0(V)$ for the Cr_3Si Debye class

The next step consists in trying to draw a relationship between the $\Theta_0(M)$ Debye classes and the $\Theta_0(V)$ behaviors. As already mentioned in the introduction, and for reasons not yet understood, it is not possible to have the same $\Theta_0(V)$ families, as compared to the $\Theta_0(M)$ classes with the exception of the $\Theta_0(M)$ Debye class of Cr_3Si. Figure 14 presents the relation $\ln\Theta_0$ as a function of $\ln V_0$ for the Cr_3Si Debye class alloys and also for the Zr-based compounds which are, surprisingly, found to fit the same straight line. The slope of this straight line is directly the Grüneisen constant 1.6 ± 0.1, which is a very reasonable value: see, for instance, Kittel,[53] who reports a list of metals and compounds for which the Grüneisen constant is between 1.25 and 2.56.

VII. DISCUSSIONS AND CONCLUSIONS

Since anharmonicity seems to be present even in the C class, it means that anharmonicity is a basic feature of each $A15$ alloy. Furthermore, one has to realize that if the thermal properties are different from one Debye class to another, it implies that

(i) The directions as well as the magnitude of the cohesive forces are not identical (a raw estimate—charge transfer—of those effects can be found in Bongi's papers[54]).

(ii) There are differences in bonding for compounds in one class as compared to alloys in another class. See Figs. 2, 3, and 4 for ECD in V_3Si, Cr_3Si, and V_3Ge.

(iii) Since the phonon spectrum depends in many ways on the bonding between atoms, it is clear that the fine structure in the phonon spectrum is different from one Debye class to another.

These three points clearly indicate that several different schemes for band structures are needed to order to explain the wide range of physical properties of the $A15$ alloys. A further consequence relates to the application of the so-called rigid-band model: in our point of view, it can at most be applied within a given class, and never between classes because of the fundamental thermal (and possibly chemical) differences.

Geller,[55] Pauling,[56] Flükiger,[40] Johnson and Douglass,[57] and Lam and Cohen,[58] seem to show that the lattice parameter of an $A15$ alloy is more the result of the B atom (see Fig. 1) than the A atom. This idea may justify the use of the ECD around the B atoms as a distinctive criterion defining Debye classes. The comparisons among the ECD of Figs. 2, 3, and 4 emphasize strongly that the important factor is the combination of a given A atom with a particular B atom. This combination determines the membership in a particular Debye class.

Another surprise from this work is the double correlation $\Theta_0(M)$ and $\Theta_0(V)$ for the C class, which represents about 20% of the binary compounds analyzed in this work. This double correspondence can be expressed in the relation $M \propto V^{-1/3}$. We have no explanation at present for this astonishing relation, considering that compounds belonging to this class have for B-atom transition metals as well as nontransition elements and composition deviations ranging from stoichiometry to $V_{0.29}Re_{0.71}$ (see Figs. 6 and 14).

The Debye classification presented here reinforces the conclusions of previous studies,[31] which have argued for a fundamental role for anharmonicity among high-T_c materials. However, we show that Nb_3Al, Nb_3Ga, and Nb_3Ge are *not* in the V class. This indicates that there is a limit to T_c enhancement by anharmonicity, possibly due to saturation effects or, perhaps, to competing processes.

Table III provides three different kinds of superconducting transition-temperature averages per Debye class. The first one concerns all compounds belonging to a given class, the second is related to alloys where all the components are transition elements only, and finally, the third regards compounds where the B part of A_3B is composed of nontransition elements. One can see that the first type of averages reflects the results of the third kind: that is, the general behavior of $\bar{T}_c$ becomes progressively lower from the V class to the C class. This means that the highest $\bar{T}_c$ average comes from the V class, the most anharmonic one. In addition, Table III shows three surprising results.

(i) There are only two alloys in the V class where the B part of A_3B is composed of transition elements, namely, Ti_3Ir and Ti_3 (Ir-Pt). This Debye class is then dominated by a mixture of transition elements (T, V, and Nb) and nontransition elements (Si, Ga, Ge, Sn, . . .).

(ii) All compounds except one in the G-C class are melted from transition elements only.

(iii) The $A15$ alloys made of transition elements only are, as one can see from Table I, scattered everywhere (with the possible exception, of the G-C class) in Fig. 6 with no apparent relationship to one another. This absence of relation is translated into an average of $\bar{T}_c \sim 4.5$ K independent of the Debye class. There are no explanations at the moment for this surprising result, that is an absence of correlation between $\bar{T}_c$ and thermal properties. This fact introduces serious questions about the usual treatment of the specific-heat data, including the McMillan[59] electron-phonon coupling parameter, for the determination of Θ_0 in about half of the $A15$ alloys.

From the phenomenology presented here, there are several different conclusions. The central role of anharmonicity suggests that correlations are strong and that the electronic band model is again inapplicable, as Brandow[60–62] has shown in several other contexts. Two or more kinds of anharmonicity, including some saturation effects, seem needed for the $A15$ compounds. We believe that the Debye classes correspond to different lattice Hamiltonians. The scatter in T_c from compound to compound in each Debye class indicates differences in the detailed dynamics and in the numerical values for coupling constants in the Hamiltonian describing the class.

One necessary consequence of the channeling experiments[63] is that the A chain distorts — the distortion being a displacive disorder. The classical equation for the bent chains is the Sine-Gordon equation. This equation has soliton solutions which form a condensate along the chains. In some cases interaction with the linear quantum modes is important, e.g., the V class, whereas the others, e.g., the C class, it is not. Perturbations due to three-dimensional effects by the environment on the chain are also interesting. The unified behavior of the transition elements in the face of their large fluctuations from member to member is extremely interesting and suggests that we should be able to improve the lattice dynamics described in Refs. 18 and 19 using the observations reported here. If so, it will be reported in a future paper.[64] Finally, not only would specific-heat data help, but additional types of data would be even more helpful, especially pressure-dependent x-ray and neutron-elastic scattering at different temperatures. The pressure dependence of Raman and infrared spectroscopic data,[65] and even thermal-expansion measurements, would be quite useful in delineating among possible models for the $A15$ compounds, although not many single crystals are available.

ACKNOWLEDGMENTS

The authors warmly thank Dr. R. M. Waterstrat for painstakingly checking all of the material in the figures and particularly in the tables. We wish also to acknowledge useful discussions with Dr. G. R. Stewart, an incisive question by Professor R. G. Barnes on the special role of transition elements, Professor C. A. Swenson for his comments on anharmonicity and specific heat measurements; and Professor C. Stassis and Professor B. N. Harmon for their encouragement. J.-L. Staudenmann thanks the Swiss National Foundation (Request No. 820.360.75) and the U.S. National Science Foundation (Grant No. PHY 76-08960). In addition, one of us (B.D.F.) was supported by the U.S. Department of Energy, Contract No. W-7605-Eng-82, Division of Engineering, Mathematical and Geosciences, Budget code AK-01-04-02. Ames Laboratory is operated for the U.S. Department of Energy by Iowa State University under Contract No. W-7405-eng-82. This research was supported by the Director for Energy Research, Office of Basic Energy Sciences, WPAS-KC-02-02-02.

*Permanent address: Department of Physics, University of Missouri, Columbia, Mo. 65211.
[1]A. L. Giorgi, B. T. Matthias, and G. R. Stewart, Solid State Commun. 27, 291 (1978).
[2]H. A. C. M. Bruning, Philips Res. Rep. 22, 349 (1967).
[3]A. Junod, J.-L. Staudenmann, J. Muller, and P. Spitzli, J. Low Temp. Phys. 3, 25 (1971).
[4]F. J. Morin and J. P. Maita, Phys. Rev. 129, 1115 (1965).
[5]L. J. Vieland and A. W. Wicklund, Phys. Rev. 166, 424 (1968).
[6]A. Junod, J. Muller, H. Rietschel, and E. Schneider, J. Phys. Chem. Solids 35, 317 (1978).
[7]P. Spitzli, R. Flükiger, F. Heiniger, A. Junod, J. Muller, and J.-L. Staudenmann, J. Phys. Chem. Solids 31, 1531 (1970).
[8]A. Junod, Thesis No. 1661 (University of Geneva, 1974) (unpublished).
[9]G. R. Stewart and A. L. Giorgi, Phys. Rev. B 17, 3534 (1978); J. Low Temp. Phys. 41, 73 (1980).
[10]J. R. Gavaler, M. A. Janocko, and C. K. Jones, J. Appl. Phys. 45, 7 (1974).
[11]L. R. Testardi, R. L. Meek, J. M. Poate, W. A. Royer, A. R. Storm and J. H. Wernick, Phys. Rev. B 11, 4304 (1975).
[12]P. Debye, Ann. Phys. (Leipzig) 39, 789 (1912); 43, 49 (1914).
[13]J.-L. Staudenmann, Thesis No. 1735 (University of Geneva, 1976) (unpublished).
[14]J.-L. Staudenmann, P. Coppens, and J. Muller, Solid State Commun. 19, 29 (1976).
[15]J.-L. Staudenmann, Solid State Commun. 23, 121 (1977).
[16]J.-L. Staudenmann (1976) (unpublished results).
[17]J.-L. Staudenmann, Solid State Commun. 26, 461 (1978).
[18]J.-L. Staudenmann and L. R. Testardi, Phys. Rev. Lett. 43, 40 (1979); 44, 553 (1980).
[19]J.-L. Staudenmann and L. R. Testardi, in *Superconductivity in d- and f-band Metals,* edited by H. Suhl and M. B. Maple (Academic, New York, 1980), pp. 247–257.
[20]B. P. Schweiss, B. Renker, E. Schneider, and W. Reichardt, in *Superconductivity in d- and f-band Metals,* edited by D. H. Douglass (Plenum, New York, 1976).
[21]A. Junod, D. Bischel, and J. Muller, Helv. Phys. Acta 52, 580 (1979).
[22]L. R. Testardi and T. B. Bateman, Phys. Rev. 154, 402 (1967).
[23]K. R. Keller and J. J. Hanak, Phys. Rev. 154, 628 (1967).
[24]G. A. Alers, in *Physical Acoustics,* edited by W. P. Mason (Academic, New York, 1965), Vol. III B, pp. 1–42.
[25]M. Rosen, H. Klimker, and M. Weger, Phys. Rev. 184, 466 (1969).
[26]R. Flükiger, J.-L. Staudenmann, and P. Fischer, J. Less-Common Met. 50, 253 (1976).
[27]B. N. Kodess, Phys. Lett. A 73, 53 (1979).
[28]A. Paoli (1975) (private communications and unpublished results).
[29]G. R. Stewart, A. L. Giorgi, and R. Flükiger, Bull. Am. Phys. Soc. 24, 426 (1979).
[30]G. D. Cody, J. J. Hanak, C. T. McConville, and F. D. Rosi, RCA Rev. 25, 338 (1964); W. Kunz and E. Saur, Z. Phys. 189, 401 (1966); S. Wada and K. Asayama, J. Phys. Soc. Jpn 34, 1168 (1973).
[31]L. R. Testardi, Rev. Mod. Phys. 47, 637 (1975), and references therein.
[32]G. Grüneisen, Handb. Phys. 10, 1 (1926); 10, 1 (1928).
[33]P. F. García and G. R. Barsch, Phys. Status Solidi B 59, 595 (1973); R. E. Larsen and A. L. Ruoff, J. Appl. Phys. 44, 1021 (1973); B. N. N. Achar and G. R. Barsch, Phys. Rev. B 19, 3761 (1979); Z. P. Chang and G. R. Barsch, *ibid.* 22, 3242 (1980).
[34]P. F. García, G. R. Barsch, and L. R. Testardi, Phys. Rev. Lett. 27, 966 (1971).
[35]B. W. Batterman and C. S. Barret, Phys. Rev. Lett. 13, 350 (1966); Phys. Rev. 145, 296 (1966).
[36]L. J. Vieland, J. Phys. Chem. Solids 33, 581 (1972).
[37]A. Junod, R. Flükiger, and J. Muller, J. Phys. Chem. Solids 37, 27, (1976).
[38]P. Spitzli, Phys. Konden. Mater. 13, 22 (1971).
[39]R. Flükiger, Thesis No. 1570 (University of Geneva, 1972) (unpublished).
[40]L. R. Testardi, T. Wakiyama, and W. A. Royer, J. Appl. Phys. 48, 2055 (1977).
[41]L. D. Hartsough and R. H. Hammond, Solid State Commun. 9, 885 (1971).
[42]D. Dew-Hughes, Cryogenics 15, 435 (1975).
[43]E. Nembach and K. Tachikawa, J. Less-Common Met. 19, 359 (1969).
[44]A. Junod, F. Heiniger, J. Muller, and P. Spitzli, Helv. Phys. Acta 43, 59 (1970).
[45]R. Flükiger, F. Heiniger, A. Junod, J. Muller, P. Spitzli, and J.-L. Staudenmann, J. Phys. Chem. Solids 32, 459 (1971).
[46]C. Susz, R. Flükiger, F. Heiniger, and J. Muller, Helv. Phys. Acta 43, 751 (1970).
[47]F. Heiniger, E. Bucher, and J. Muller, Phys. Konden. Mater. 5, 263 (1966).
[48]G. R. Stewart, L. R. Newkirk, and F. A. Valencia, Phys. Rev. B 20, 3647 (1979).
[49]B. Cort, G. R. Stewart, C. L. Snead, Jr., A. R. Sweedler, and S. Moehlecke (unpublished).
[50]R. H. Willens, T. H. Geballe, A. C. Gossard, J. P. Maita, G. W. Hull, Jr., and R. R. Soden, Solid State Commun. 7, 837 (1969).
[51]G. R. Stewart, E. G. Szklarz, and A. L. Giorgi, Solid State Commun. 28, 5 (1978).
[52]K. Bohmhammel, G. Wolf, N. E. Alekseevskii, and E. P. Krasnoperov, Solid State Commun. 21, 519 (1977).
[53]C. Kittel, *Introduction to Solid State Physics,* 3rd ed. (Wiley, New York, 1968); the same table can also be found in G. Busch and H. Schade, *Lectures on Solid State Physics* (Pergamon, Oxford, 1976).
[54]G. H. Bongi, Thesis No. 1692 (University of Geneva, 1975) (unpublished).
[55]S. Geller, Acta Crystallogr. 9, 885 (1956); 10, 380 (1957).
[56]L. Pauling, Acta Crystallogr. 10, 374 (1957); 10, 685 (1957).
[57]G. R. Johnson and D. H. Douglass, J. Low Temp. Phys. 14, 565 (1974).
[58]P. K. Lam and M. L. Cohen, Phys. Lett. A 81, 457 (1981).
[59]W. L. McMillan, Phys. Rev. 167, 331 (1968).
[60]B. H. Brandow, Phys. Rev. B 12, 3464 (1975).
[61]B. H. Brandow, Int. J. Quantum Chem. Symp. 10, 417 (1977).
[62]B. H. Brandow, Adv. Phys. 26, 651 (1977).
[63]L. R. Testardi, J. M. Poate, W. Weber, W. M. Augustyniak, and J. H. Barnett, Phys. Rev. Lett. 39, 716 (1977).
[64]B. DeFacio and J.-L. Staudenmann (unpublished).

[65]W. F. Sherman, J. Phys. C 13, 4601 (1980), and references therein.
[66]C. C. Huang, A. M. Goldman, and L. E. Toth, Solid State Commun. 33, 581 (1980).
[67]A. Handstein, Phys. Status Solidi B 95, 131 (1979).
[68]R. Flükiger, P. Spitzli, F. Heiniger, and J. Muller, Phys. Lett. A 29, 407 (1969).
[69]G. R. Stewart and A. L. Giorgi, Solid State Commun. 26, 665 (1978).
[70]G. R. Stewart, L. R. Newkirk, and F. A. Valencia, Phys. Rev. B 21, 5055 (1980).
[71]G. R. Stewart and G. W. Webb, Solid State Commun. 33, 1015 (1980).
[72]C. C. Tsuei, S. von Molnar, and G. M. Coey, Phys. Rev. Lett. 41, 664 (1978).
[73]R. Flükiger, A. Paoli, R. Roggen, K. Yvon, and J. Muller, Solid State Commun. 11, 61 (1972).